Table 1. Products of hydrolysis of rhapidosome RNA (seven strains) for 18 hours at 35°C in 0.5*N* KOH. Abbreviations: O.D., optical density; ONT, oligonucleotides; MNT, mononucleotides; CMP, cytidine monophosphate; AMP, adenosine monophosphate; GMP, guanosine monophosphate; UMP, uridine monophosphate.

Strain	Percentage of O.D. at 260 nm		Base distribution of MNT released (mole %)			
	ONT	MNT	CMP	AMP	CMP	UMP
WH	97	3	55			45
Daw-2	93	7	52	3	7	38
Gol-12	75	25	36	25	22	17
Jl-4	88	12	50	14	9	27
Si-09	95	5	39	12	23	26
Eg-13	86	14	47			53
Lim-21	40	60	17	11	25	47

In the case of *S. grandis* RNA, the soluble and ribosomal fractions were combined and enzymically hydrolyzed for freeing of nucleosides; the methylated fraction of nucleosides was separated from the nonmethylated fraction by zone electrophoresis in borate buffer, and the two fractions were eluted with dilute HCl for absorption measurements at 260 nm (*2*).

The methylated fraction of nucleosides was too small for detection by these methods (less than 5 percent); thus the bulk of the soluble and ribosomal RNA from *S. grandis* cells was not highly methylated and was different in type from the RNA isolated from the rhapidosomes. Rhapidosome RNA fractions from DEAE-cellulose chromatography were dialyzed against distilled water, concentrated with a flash evaporator, and hydrolyzed in 0.5*N* KOH at 35°C for 18 hours. The hydrolyzates were neutralized in the cold with $HClO_4$, and the $KClO_4$ that formed was removed by centrifugation at 0°C.

The fractions were then applied to fresh DEAE-cellulose columns (2.5 by 35 cm) which were eluted as before hydrolysis. Free nucleotides or dinucleotides, which were eluted early in the gradient, were applied to a Dowex-1-10X-formate column (1.2 by 30 cm). The Dowex-1 columns were eluted (*8*), and fractions were tested for absorption at 260 nm. Absorption spectra and orcinol (*9*) assays were routinely measured for all column fractions in which absorption at 260 nm was found. 2′-*O*-Methyl ribose gives approximately the same orcinol assay per mole as does ordinary ribose (*9*).

All seven rhapidosomes contained RNA that was always highly 2′-*O*-methylated (Table 1). The 2′-*O*-methyl group confers stability to alkaline hydrolysis only to the phosphodiester linkage at the 3′-position of the methylated nucleotide. Mononucleotides that are released must be nonmethylated themselves and must also be linked at the 5′-position to another nonmethylated nucleotide. The mononucleotides released from the RNA of the rhapidosomes varied in base distribution from strain to strain and were nonrandom. In some instances the nucleotides released were almost exclusively pyrimidine nucleotides. If a single methylated nucleotide is found within a nonmethylated portion of the chain, a dinucleotide will be released by alkaline hydrolysis. Only traces (less than 1 percent) of such dinucleotides were found in any of the seven rhapidosome RNA hydrolyzates.

I conclude that flexibacterial rhapidosomes constitute a class of particle that contains an RNA that is unusual in that it is highly but not completely 2′-*O*-methylated. The distribution of this methylation along the RNA chains and among the nucleotides of the chains is nonrandom and varies from strain to strain.

DAVID L. CORRELL
Radiation Biology Laboratory,
Smithsonian Institution,
Washington, D.C. 20560

References and Notes

1. R. A. Lewin, *Nature* **198**, 103 (1963); R. E. Reichle and R. A. Lewin, *Can. J. Microbiol.*, in press.
2. D. L. Correll and R. A. Lewin, *Can. J. Microbiol.* **10**, 63 (1964).
3. H. Reichenbach, *Arch. Mikrobiol.* **50**, 246 (1965).
4. W. Van Iterson, J. F. Hoeniger, E. N. Van Zanten, *J. Cell Biol.* **32**, 1 (1967).
5. Y. I. Rautenstein, S. B. Stefanov, E. I. Smirnova, L. N. Khadji-Murat, *Microbiologia* **30**, 860 (1966).
6. Flexibacterial cultures were obtained from R. A. Lewin, Marine Biology Department, Scripps Institution of Oceanography, La Jolla, Calif.
7. D. L. Correll and N. E. Tolbert, *Plant Physiol.* **37**, 627 (1962).
8. D. L. Correll, *Plant Cell Physiol.* **6**, 661 (1965).
9. ———, *Phytochemistry* **4**, 453 (1965).

10. Aided by Smithsonian Research Foundation grant 58-0001-3357. Publication by approval of the secretary, Smithsonian Institution.

17 May 1968

Rupture Mechanism of a Liquid Film

Abstract. *The rupture mechanism of edge-supported liquid films appears to involve the viscous and drag energies as well as previously postulated kinetic and surface energies. Although details are obscure, the mechanism appears to involve a liquid-gathering process at the free edge, followed by fragmentation of this thickened edge into drops whose radii are approximately 50 times the film's original thickness.*

Little work has been reported concerning the processes occurring during the collapse of a liquid film. Dupre (*1*), who was the first to study the film-rupturing process, calculated the speed at which a liquid film ruptures by assuming that the surface energy of the film is completely converted into the kinetic energy of the liquid according to the relation

$$2\,\nu S = \tfrac{1}{2}\,S\lambda\rho V^2 \qquad (1)$$

where ν is the surface tension of the film in dynes per centimeter, S is the total surface area of the film in square centimeters, λ is the film thickness in centimeters, ρ is the liquid density in grams per cubic centimeter, and V is the velocity of the retracting edge in centimeters per second. Rayleigh (*2*) and Devries (*3*) studied the rupturing of soap films formed on circular wire frames and measured rupture velocities of 350 to 1500 cm/sec. The work of Devries indicates that the rupture velocity remains constant during the entire process, which suggests that the phenomena quickly attain a steady state. Droplet formation during film rupture apparently was not observed by these investigators, and the film thicknesses were not reported; thus it is difficult to assess the suitability of Dupre's relation. It would appear, however, that this equation can only give an upper limit for the velocity of the free edge of the film, since such dissipative forces as drag and viscosity were neglected. While studying the bursting of bubbles at liquid-air interfaces, other investigators (*4*) noted the formation of a fine spray of drops at the instant of burst.

This report describes our investigation of the processes occurring in the vicinity of a free edge during film rupture. In our experiments we used flash (8 μsec) photography, flash interferometry, and high speed (5000 frame/

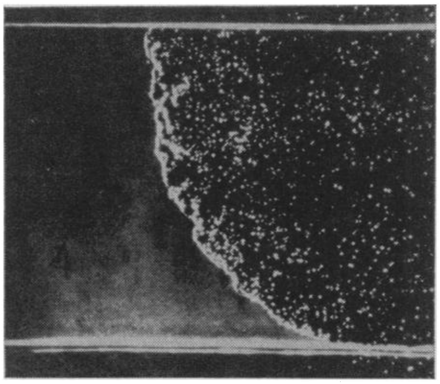

Fig. 1. Flash photograph of the rupturing front of a vertically positioned liquid lamella collapsing from right to left; 0.65 times normal size.

sec) photography. The films were prepared from an aqueous solution containing 15 percent (by volume) commercial liquid detergent and 15 percent (by volume) glycerol and were formed on rectangular wire frames either 3.8 or 6.4 cm wide and 20 cm long. The film was perforated near one end of the frame, and the free edge was photographed after it had traversed approximately one-half the length of the frame. A flash photograph (Fig. 1) of the free edge of a vertically mounted film (collapsing from right to left) shows a roughened and highly irregular edge with numerous liquid drops attached to the film edge and in its wake. Vertically positioned films show a nonuniform thickening of the film from top to bottom due to the fluid motion impelled by gravity. In Fig. 1, the rupturing film front is curved, showing the influence of film thickness on the rupturing velocity; the thinner, upper portion of the film retracts at a higher velocity than the lower, thicker part does. Similar photographs of horizontally positioned films showed that some of the drops separating from the edge have vertical velocity components, which give rise to divergent dispersion patterns.

A flash interferogram of a rupturing vertical lamella is shown in Fig. 2a. The straightness of the interference fringes on the right (lamella) side signifies a uniform, horizontal film thickness and indicates that the rupturing process does not cause film thickening at distances from the free edge. Gravitationally induced film thickening is illustrated by the progressive vertical increase in fringe spacing. The relative thickness of the film at the far right side of the photograph was calculated from measurements of fringe spacing (Fig. 2b). The absolute film thickness at the top of the film frame was not directly measurable from the interferogram. Fringe curvature, in the proximity of the free edge, is indicative of a horizontal thickening of the lamella with approach of the edge. Thickness of the film adjacent to the free edge is shown in Fig. 2b. Close irregular clusters of drops attached to the film's free edge (Fig. 1) obscure the fringe pattern and make it difficult to discern the shifts at the edge. The narrow region of film at the edge, influenced by the rupturing front, appears to increase with increased film thickness; at the top of the film frame, lamella thickening begins a few millimeters in advance of the free edge, whereas at lower levels and with thicker film, thickening is apparent at distances greater than 1 cm from the advancing front.

Table 1. Summary of conditions and results in liquid lamella rupturing experiments.

Surface tension at 21°C (dyne/cm)	Film thickness (μm)	Film rupture velocity (cm/sec)	Drop radius(μm) Minimum	Drop radius(μm) Maximum	Drop radius(μm) Average	Film surface energy (erg/cm²)	Kinetic energy (erg/cm²)
28	0.58	880	25	70	40	56	23
28	0.87	730	32	80	55	56	23
28	1.16	620	38	62	50	56	22

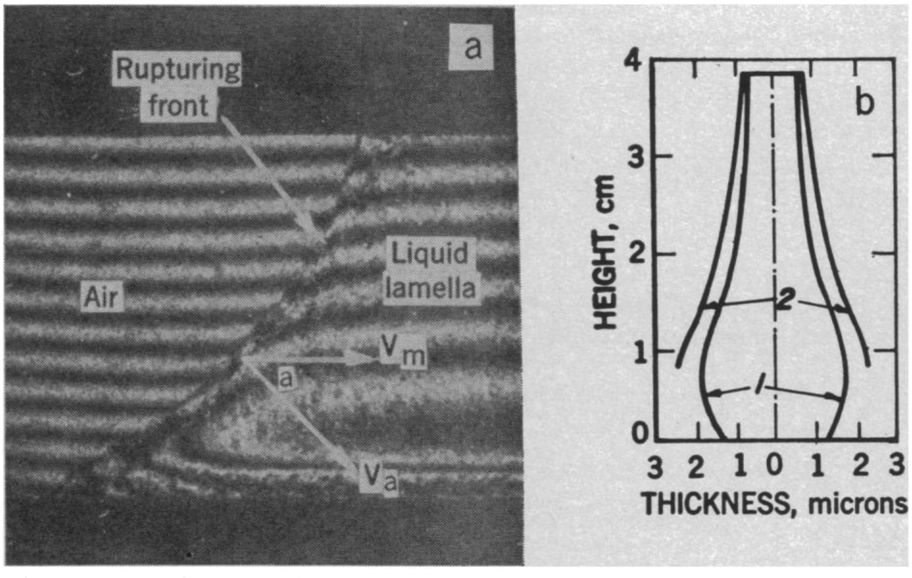

Fig. 2. (a) Interferogram of a vertical liquid lamella rupturing from left to right. (b) Thickness profile of the lamella (1) at the far right side of the interferogram and (2) adjacent to the rupturing front.

The rupturing front in Fig. 2a has traveled approximately 10 cm from the initial perforation and appears to be propagating without change in shape. The shape of this edge, if Dupre's relationship is correct, should be a result of the dependency of the normal velocity of the grathering edge, V_a, on the changing film thickness. Later experiments demonstrated that the free edge retracts in a direction normal to its tangent vector and that the configuration as a whole moves from left to right at a constant velocity, V_m. Accordingly, the normal edge velocity is $V_a = V_m \cos a$, where a is the angle subtended by the two velocity vectors as shown in Fig. 2a. The film thickness can be expressed as a function of velocity by rearrangement of Dupre's equation (*1*) as follows:

$$\lambda_a = K/V_a^2 \qquad (2)$$

where K is a constant equal to $4\nu/\rho$. This relation indicates that the thinnest portion of the film edge has the maximum normal velocity; this velocity consequently determines the horizontal velocity of the configuration. We had no direct measurement of the film thickness since interferometric techniques measure only the relative change in thickness. However, by subtracting from Eq. 2 a similar equation for the thinnest portion of the film we obtain the relation:

$$\lambda_a - \lambda_m = K/V_m^2[(V_m/{}_a)^2 - 1] \qquad (3)$$

where $\lambda_a - \lambda_m$ is the difference in film thickness between any arbitrary cross section having a normal angle a and the thinnest portion λ_m, and V_m and V_a are the corresponding normal velocities; V_m is the horizontal or configurational velocity. If Dupre's relationship is correct, the quality $\lambda_a - \lambda_m$ (determined from the interferometric patterns, assuming a refractive index of 1.33 for the film) plotted against $(V_m/V_a)^2$ should fit a straight line having a slope of K/V_m^2 and an intercept of $-K/V_m^2$. These results are plotted in Fig. 3. The linearity of the line indicates that Dupre's assertion (that the kinetic energy of the film is constant and independent of film thickness) is apparently correct. However, additional mass-independent energies which result from the dissipative forces of drag and viscosity can be added to Eq. 1 without affecting Eq. 3. Furthermore, since $V \rightarrow \infty$ or $V^{-1} \rightarrow 0$ as $\lambda_a \rightarrow 0$, the intercept of the line with the ordinate corresponds to λ_m, the minimum film thickness. For this particular experiment λ_m appears to be about 1.1 μm.

Studies of high-speed photography were conducted with horizontally positioned films. An analysis of these photographs shows that the rupturing edge contracts in a direction normal to the tangent of the film edge and at a velocity which is essentially constant for a given film thickness. Drops formed at the rupturing edge free themselves from the film and continue to move in the same direction and initially at the same velocity as the rupturing front. The high-speed framing experiments also provided additional data to test Dupre's energy relationship, namely, to determine if kinetic and surface energies are the only energies responsible for the film motion. Table 1 lists the conditions and results of three high-speed framing experiments with different film thicknesses. The light-interference techniques described by Bikerman (*5*) were used to visually measure the film thickness prior to rupture.

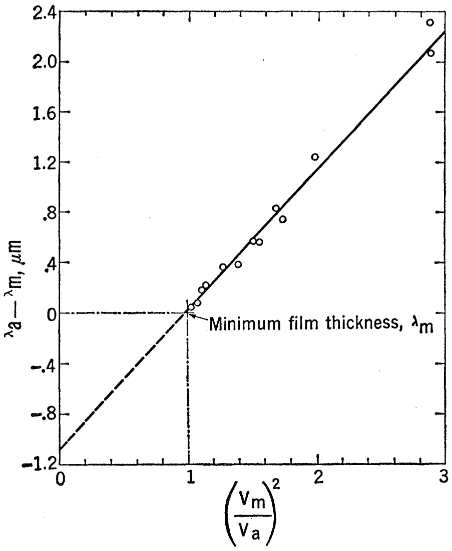

Fig. 3. Difference in thickness of a vertical film at any height (λ_a) and the lamella at the top of the film frame (λ_m) as a function of the square of the ratio of the horizontal film rupturing velocity to the normal velocity.

The sizes of the drops formed during film rupture were estimated by measuring the aerodynamic drag on the drops after release from the film. The force equation of a spherical drop of radius r moving at a velocity V through a quiescent atmospheric environment is:

$$M\,dV/dt + c/2\,A\rho_a V^2 = 0 \qquad (4)$$

where M is the drop mass ($4/3\,\pi r^3 \rho_l$), ρ_l and ρ_a are the liquid and air densities, A is the cross-sectional area of the drop (πr^2), t is the time, and c is the drag coefficient [18.5 $\mathrm{Re}^{-0.6}$ (*6*), where Re is the Reynolds number ($2\,rV\rho_a/\mu_a$) and μ_a is the air viscosity]. The first term in Eq. 4 is the inertial force of the drop and the second is the viscous drag of the air on the drop. Integrating Eq. 4 for the distance of drop travel, x, yields:

$$x = (2/3K)\,[V_0^{0.6} - (V_0^{-0.4} + kt)^{-3/2}] \qquad (5)$$

where

$$K = 2.78\ \rho_a/\rho_l(\mu_a/2\rho_a)^{0.6} r^{-1.6} \qquad (6)$$

and V_0 is the drop velocity at the time of separation from the film ($t = 0$). Drop sizes were estimated from Eq. 5 to fit the experimental data of drop position against time of travel. Owing to the vertical velocity component of some of the drops, only those that remained in focus (the depth of field was approximately 6 mm) and whose trajectories remained normal to the rupturing front were used. Drop radii so determined are shown in Table 1, where the minimum, maximum, and average drop radius for each experiment are indicated. Radii for from seven to ten drops were determined for each experiment. Comparison of the film-rupturing velocity and film thickness shows that film-rupturing velocity decreased with increasing film thickness in accordance with Dupre's relationship.

The values for kinetic energy shown in Table 1 correspond to the kinetic energy of the film, that is, the product of one-half the square of the velocity of the free edge and the mass per unit area of the film far removed from the edge. It has been shown that the velocity of the free edge equals the initial velocity of the drops; therefore, this latter energy is also the initial kinetic energy of the free drops ultimately to be dissipated in aerodynamic drag. The similar values for kinetic energy obtained for the three experiments confirm the previous results of the interferometric study, that the kinetic energy is constant and independent of film thickness. However, a comparison of the film surface and kinetic energy values in Table 1 indicates that these results are not in accord with Dupre's relationship (Eq. 1) since the kinetic energy accounts for only 40 percent of the available film energy.

In view of our results, the surface energy of the film is assumed to be converted into: (i) kinetic energy of the film's free edge; (ii) dissipative energies resulting from environmental drag and internal liquid viscosity, which are involved during the thickening process at the free edge; and (iii) surface energy of the drop. The energy dissipated in drag forces during the rupturing process is approximately 8 percent of the total available surface energy of the film. In addition, the surface energy which remains on the drops is about 2 percent of the available energy. If these energies are added to the kinetic energy value of 40 percent, it follows that the remaining energy, which can be attributed to internal viscous forces, is approximately 50 percent of the total energy of the film surface.

ISRAEL LIEBMAN
JOHN CORRY
HENRY E. PERLEE

Bureau of Mines,
U.S. Department of the Interior,
Pittsburgh, Pennsylvania

References

1. A. Dupre, *Theorie Mecanique de la Chaleur* (Gauthier-Villars, Paris, 1869), p. 350.
2. B. Rayleigh, *Sci. Papers Cambridge* **3**, 441 (1903).
3. A. J. Devries, *Rec. Trav. Chim.* **77** (part 4), 383 (1958).
4. R. L. Aspden, *Roy. Aircraft Estab. Tech. Note Inst.* **141**, (Ministry of Supply, London, 1952); D. M. Newitt, N. Dombrowski, F. H. Knelman, *Trans. Inst. Chem. Engrs. London* **32**, 244 (1954).
5. J. J. Bikerman, *Foams: Theory and Industrial Applications* (Reinhold, New York, 1953), p. 138.
6. R. B. Bird, W. E. Stewart, E. N. Lightfoot, *Transport Phenomena* (Wiley, New York, 1965), p. 192.

10 June 1968